Closed-loop learning control of isomerization using shaped ultrafast laser pulses in the deep ultraviolet

Marija Kotur,[1] Thomas Weinacht,[1,a)] Brett J. Pearson,[2] and Spiridoula Matsika[3]
[1]*Department of Physics, Stony Brook University, Stony Brook, New York 11794, USA*
[2]*Department of Physics and Astronomy, Dickinson College, Carlisle, Pennsylvania 17013, USA*
[3]*Department of Chemistry, Temple University, Philadelphia, Pennsylvania 19122, USA*

(Received 15 October 2008; accepted 2 March 2009; published online 6 April 2009)

We demonstrate the use of shaped ultrafast laser pulses in the deep ultraviolet to control the ring opening isomerization of 1,3-cyclohexadiene to form 1,3,5-hexatriene. The experiments are performed with a gas phase sample and the isomerization yield is probed with dissociative ionization driven by a time-delayed, intense infrared laser pulse. Differences in the electronic structure of the ions for the two isomers, as shown by *ab initio* calculations, result in very different fragmentation products following strong-field ionization. We find that a shaped pulse yields a ~37% increase in the isomerization over an unshaped laser pulse. © *2009 American Institute of Physics*. [DOI: 10.1063/1.3103486]

I. INTRODUCTION

Isomerization plays a crucial role in fundamental processes such as vision and combustion and there is substantial interest in controlling isomerization from the perspective of molecular switches.[1–7] Recent experiments demonstrated learning control[8] of isomerization in the liquid phase[9–12] using shaped ultrafast laser pulses. However, solvent interactions and nonlinear optical effects, which are prevalent in experiments performed in liquids, make interpretation of these control experiments difficult.[13] Mass-resolved, particle-detection based control experiments performed in the gas phase serve as important complements to liquid phase experiments in trying to understand the underlying control mechanisms. Indistinguishability of the time-of-flight mass spectra (TOFMS) of different isomers has to date been a hindrance to such experiments. Differences in the TOFMS of 1,3-cyclohexadiene (CHD) and its isomer 1,3,5-hexatriene (HT) following strong field ionization with infrared laser pulses[14] enable the detection of distinct isomers necessary for producing an experimental feedback signal.

The accepted picture of isomerization driven by UV absorption in CHD[14–20] involves launching a wave packet from the ground $1A_1$ state of CHD to the one-electron excited $1B_2$ state. The wave packet, driven by the slope of the $1B_2$ potential, evolves in the direction of a conical intersection (CI) between the $1B_2$ and the two-electron excited state $2A_1$, and crosses over to the $2A_1$ surface. Its evolution on this surface drives it toward a second CI with the ground state. Solution-phase measurements show that in passing through the CI to the ground state, the wave packet bifurcates, with about 40% going toward a minimum in the ground state corresponding to HT and 60% going toward the minimum corresponding to CHD.[21]

Figure 1 illustrates our experimental approach. A shaped UV pulse excites the molecule, launching a wave packet on

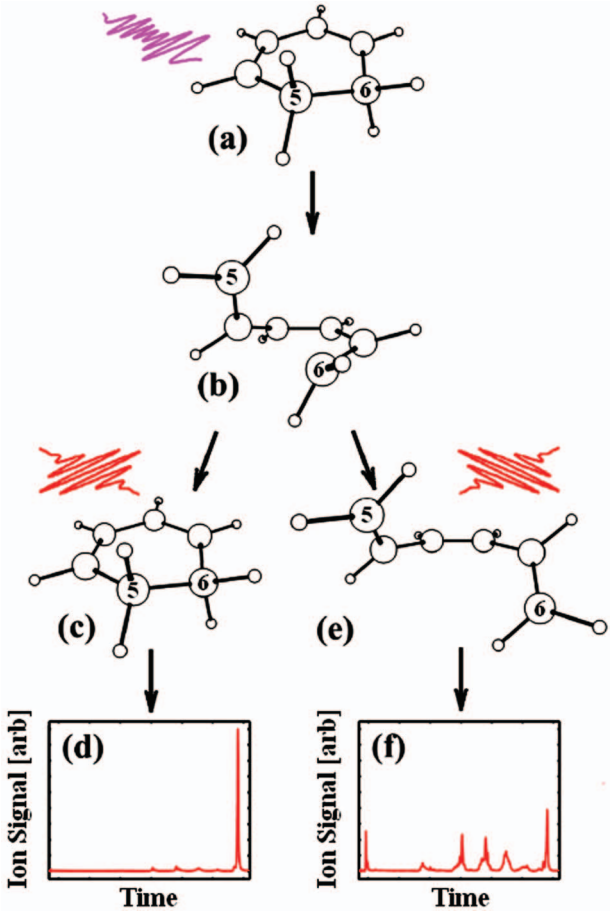

FIG. 1. (Color) Cartoon of the experimental approach: The experiment starts with a shaped UV pulse interacting with the molecule initially in the CHD conformation (a). Following UV excitation it evolves toward a CI (b) after which it can become CHD again (c) or undergo ring opening to become HT (e). Subsequent IR ionization leads to pronounced differences in the TOFMS for the two isomers (d) and (f). The geometries shown were derived by *ab initio* calculations and the two TOFMSs were measured on raw samples and presented here on the same vertical scale. Carbon atoms C^5 and C^6 are labeled in appropriate panels.

a)Electronic mail: tweinacht@sunysb.edu.

the $1B_2$ state [Fig. 1(a)]. The wave packet evolution on this state leads to a CI with a geometry shown in Fig. 1(b). Bifurcation of the wave packet at the CI leads to the production of CHD [Fig. 1(c)] or cZc-HT, the HT conformer likely to be reached first in the ring-opening reaction [Fig. 1(e)]. We are able to distinguish whether the molecule ends up as CHD or HT after going through the second CI by illuminating the sample with an intense IR probe pulse approximately 1.8 ps after the shaped UV pump. As shown in the panels of Figs. 1(d) and 1(f), the strong IR pulse produces very different fragment yields for HT compared to CHD.

II. EXPERIMENT

The core of our experimental setup is an amplified Ti:sapphire laser producing 30 fs pulses with a central wavelength of 780 nm, repetition rate of 1 kHz, and energy of 1 mJ. We generate pulses at 260 nm by first producing light at the second harmonic of our laser in a beta-BaB_2O_4 crystal and then using sum frequency generation of the second harmonic and fundamental to generate the third harmonic. We make use of a calcite crystal for group velocity mismatch compensation and the nonlinear crystals are placed in a diverging beam following a focus in vacuum in order to optimize the conversion efficiency and mode quality. After tripling, we have 17 μJ of 260 nm, sub-50 fs ultraviolet light and 250 μJ remaining in the fundamental.

The UV and IR pulses are separated using a dichroic mirror and sent into a Mach–Zender interferometer. One arm of the interferometer contains a computer controlled, acoustic-optic modulator based ultraviolet pulse shaper,[22] while the other arm contains a prism-based dispersion-compensating delay line.[23,24] The UV pulses are characterized by self-diffraction frequency resolved optical gating.[25] The unshaped UV pulses are close to transform limited with a pulse duration of about 50 fs.

The UV and IR beams are collinearly recombined using a dichroic mirror and focused by a 150 mm fused silica lens into an effusive molecular beam inside a vacuum chamber. Since the lens has a longer focal length for the IR than for the UV, we make use of an additional pair of lenses in the IR beam to produce a slightly converging beam before the shared focusing lens.

Molecular fragment ions are directed into a time-of-flight mass spectrometer with a dual slope extraction configuration. The field-free region of the TOFMS provides a temporal separation of different ions, resulting in a mass-resolved signal that is detected by a digital oscilloscope interfaced with the computer that controls the pulse shaper. This allowed for the implementation of closed-loop learning control, where the feedback signal is the yield of a selected fragment associated with HT. Details regarding the learning algorithm we used are given in.[26]

III. CALCULATIONS

First the ground states of both CHD and cZc-HT and their ions were optimized at the MP2 level using the 6–31G(d) basis. Constrained optimizations at the UHF/6–31G(d) level were carried out for the ground cationic state,

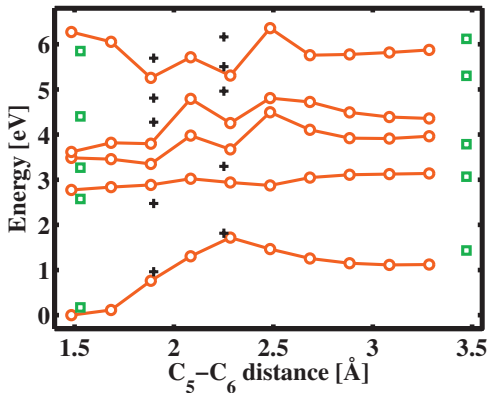

FIG. 2. (Color) Circles and lines: MCQDPT2(8,10) calculation of the lowest five energy levels of CHD^+/HT^+ for a relaxed potential energy scan along the C^5–C^6 bond length. Squares: energies of CHD^+ and HT^+ at the equilibrium geometries of the neutral CHD (left side) and HT (right side), respectively. Crosses: five lowest energy levels for the cation at the geometries corresponding to the CIs in the neutral.

where the C^5–C^6 distance was kept constant, while the other coordinates were relaxed. Energies of the ground and the first four excited states were calculated for these intermediate geometries at the multiconfigurational self-consistent field (MCSCF) and quasidegenerate multiconfigurational second order perturbation theory (MCQDPT2) (shown in Fig. 2) levels with the same basis. An active space of eight electrons in ten orbitals [denoted as (8,10)] was used in these calculations. The active space included all π and selected σ orbitals, which participate in some excited states of the cation. The constrained minimizations provide a reaction pathway between HT and CHD cations.

We also calculated the excited cationic states at selected geometries of the neutral photo-initiated reaction, corresponding to the two CIs that have been reported before as important intermediates along the reaction path.[18,19] The minimum energy points on the seam of the CIs between the first and second excited states S_2-S_1 and the ground and first excited states S_1-S_0 were calculated using a small multireference configuration interaction (MRCI) expansion with a reference space of six electrons in six orbitals (6,6) and single excitation configurations out of this active space. The COLUMBUS suite of programs was used for the CI optimizations[27,28] while GAMESS[29]) was used for all other calculations.

IV. EXPERIMENTAL RESULTS

In order to determine the optimal pump-probe delay for performing the closed-loop control experiments, we measured the fragment ion yields as a function of pump-probe delay. Figure 3 shows the $C_2H_2^+$ (a rough measure of the HT formed by the pump pulse) and parent ion yields as a function of time delay between the ultraviolet (pump) and infrared (probe) pulses. These results demonstrate the dramatic changes in the fragmentation pattern of the molecule following irradiation with an ultrafast pulse at $\lambda_0=260$ nm. The parent yield decreases when the IR pulse follows the UV pulse, while the $C_2H_2^+$ yield increases substantially. Note that the parent ion yield peaks when the two beams are spatially

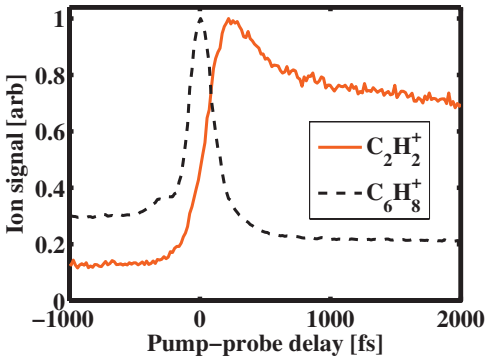

FIG. 3. (Color) $C_2H_2^+$ and parent ion yields as a function of pump-probe delay. The signals are individually normalized to their maximum values.

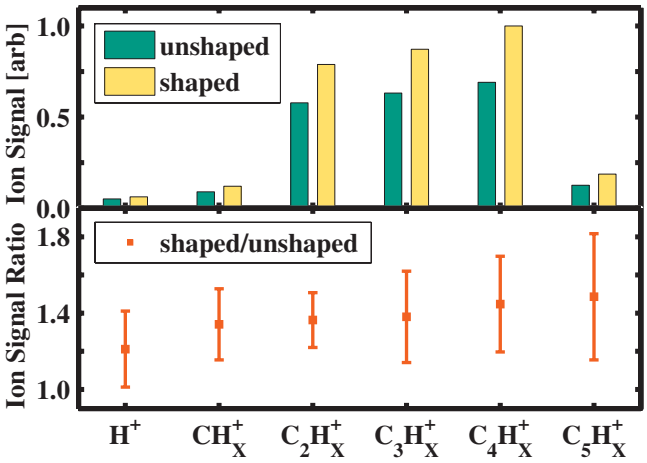

FIG. 4. (Color) Top panel: peak integrals with the unshaped and the shaped pulse (UV background subtracted). Bottom panel: shaped/unshaped peak integral ratios.

and temporally overlapped. The increase in $C_2H_2^+$ yield is delayed with respect to this peak, consistent with the time required for isomerization to take place.[14] The peak in the $C_2H_2^+$ signal after zero time delay is likely due to the wave packet passing through a location with a single IR photon resonance in the ion as the ring opening proceeds (as shown in Fig. 2). Ionization when the wave packet is at this location can lead to efficient excitation of the ion and thus additional fragmentation.[30] However, even for positive time delays after the peak in the $C_2H_2^+$ yield, there is substantial $C_2H_2^+$ produced by the IR pulse. The TOFMS for positive time delays shows a general trend of enhancing smaller molecular fragments at the expense of the parent, as one would expect with the formation of HT. Based on the pump-probe data, a delay of 1800 fs was chosen so that the control experiments would be performed after the transient signals have passed. The pulse intensities were ≤ 10 and ~ 46 TW/cm^2 for the UV pump pulse and IR probe pulse, respectively.

We found that control was sensitive to the intensity of our UV pulses and that we were only able to control the ring opening when there was sufficient UV intensity to ionize the molecules. Therefore, we took care to isolate the contributions of the pump and probe pulses to the total ion signal. With the IR probe pulse alone, the vast majority (95%) of the detected ion signal from CHD is the parent ion. After excitation with the UV pump pulse, the IR probe produces a substantial amount of lighter fragments ions (35% of the total signal). In order to determine how much of this increase is due to newly created HT molecules, we examine the ion signal from the UV pump pulse alone. In addition to creating a wave packet on the $1B_1$ state, the UV pump pulse produces some ionization and dissociation (approximately 10%–35% of the cooperative UV+IR signal for the fragment ions, 80% for the parent at full UV energy). Since these ions come from molecules that did not undergo internal conversion from CHD to HT, they need to be subtracted from the cooperative ion signal. In pump-probe experiments with the shaped pump, the shaped UV alone signal is subtracted from the cooperative signal for each pulse shape.

Figure 4 shows results from a typical pump-probe feedback control experiment of the CHD to HT isomerization reaction. The peaks in the TOFMS have been grouped according to the number of carbon atoms they contain. The bars in the top panel show the UV-background-subtracted peak integrals obtained in pump-probe experiments with both shaped and unshaped UV pulses. The bottom panel shows the ratio of these peak integrals. The error bars in the bottom panel indicate the standard deviation in the ratio among three different measurements. All the fragment signals show a clear increase with shaped pump pulse, ranging between 21% and 49% relative to an unshaped pulse. The average increase relative to the unshaped pulse is $37\% \pm 10\%$.

We note that while our measurements yield a 37% increase in the isomerization yield due to pulse shaping, they do not provide an independent measure of the absolute efficiency for either a shaped or unshaped pulse. This is due to the imperfect spatial overlap of the pump and probe pulses and the difficulty in determining the number of molecules in the interaction region.

V. DISCUSSION

The differences in the CHD and HT TOFMS can be understood in terms of the ionic spectra for the two geometries.[14] Figure 2 shows the energies of the first few ionic states of the molecule as a function of the length of the bond between atoms C^5 and C^6, whose lengthening and breaking are involved in the isomerization. The circles and lines show the ionic energies for ionic optimized geometries where the C^5–C^6 bond is constrained. The squares show the ionic energies at the equilibrium neutral geometries, CHD at the left, and HT at the right of the figure. The crosses show the ionic energies at the geometries of the CI of the neutral, S_2-S_1 CI at C^5–C^6=1.9 Å and S_1-S_0 CI at C^5–C^6=2.3 Å.

In CHD^+, the energy gap between the ground and first excited states is about 3 eV, whereas the gap for HT is about 2 eV. The calculations agree with the measured gap from photoelectron spectra in HT (1.97 eV)[31,32] and previous calculations.[33] The likelihood of HT being produced in a vibrationally hot state further reduces its effective ionization potential. As tunnel ionization is very sensitive to the effective ionization potential,[34] the smaller energy gap between the ground and first excited states of HT^+ leads to population of excited ionic states during tunnel ionization in the strong

IR pulse, whereas the larger gap in CHD^+ leads primarily to excitation of the ground ionic state. Once the first excited state of the ion is reached, population can be rapidly distributed to higher ionic states since there is a high density of states with spacings of the order of the probe photon energy (1.6 eV).

Figure 2 also shows that resonances with the IR pulse can be achieved during the ring opening. Specifically at the geometry of the CI between the ground and first excited state of neutral CHD, which is responsible for the isomerization, the gap between the ground and first excited state of the cation is ~1.5 eV. This resonance may be responsible for increased fragmentation at very short times (as seen in Fig. 3). While different conformational isomers of HT are accessible from the CI, no significant differences in their fragmentation patterns have been found,[14] allowing us to observe and quantify the isomerization of CHD without considering their effects.

There are many possible mechanisms by which a shaped pulse can control the isomerization yield. Here we discuss a few of these mechanisms, leaving a detailed analysis and determination of the control mechanism for a forthcoming publication. Three different possibilities which we considered involve manipulation of the wave packet at three different times during its evolution—the first during the wave packet launch, the second as the wave packet nears the CI, and the third as the portion of the wave packet that did not lead to isomerization reaches the CHD minimum.

A first possible mechanism involves controlling the wave packet momentum as it is formed on the $1B_2$ potential surface with a shaped excitation pulse. This could be achieved via a pump-dump-pump scheme and leads to control over the momentum of the wave packet as it crosses the S_1-S_0 CI, influencing the CHD/HT branching ratio at the CI.[11,35]

A second possibility consists of strong-field dressing the PESs to change the wave packet evolution in the vicinity of the CI. While the time required for the wave packet to travel from the Frank–Condon region of the $1B_2$ potential to the S_1-S_0 CI ($1B_2/1A_1$) [~130 fs (Ref. 14)] is longer than the duration of an unshaped pump pulse, any shaping can increase its duration so that the UV field is still present when portions of the wave packet pass near or through the CI. However, the large detuning of the UV pulse from both the $2A_1$-$1B_2$ and $2A_1$-$1A_1$ energy separations near the CI should result in weak dynamic Stark shifts and thus leads us to suspect that this mechanism is largely not responsible for the control.

A final possibility we consider is wave function "recycling." As the time constant for the wave packet relaxation from the Frank–Condon region on the $1B_2$ to the $1A_1$ potential is ca. 200 fs,[14] portions of the wave packet excited by earlier parts of the pump pulse may have returned to the ground state as later parts of the pulse arrive. Thus the part of the wave function that comes back to the CHD minimum could be re-excited by the same pump pulse and have another chance of making it to the HT minimum.[12] Such repumping could be repeated several times, in principle transferring the entire population to the HT side of the barrier.

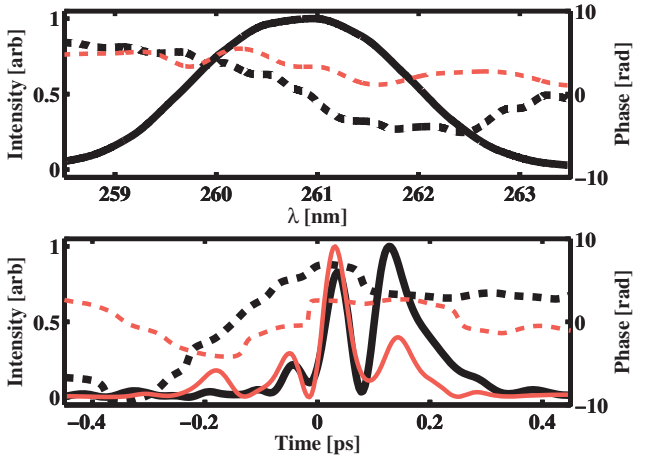

FIG. 5. (Color) Top panel: Spectral phases and corresponding spectral intensities of two of the optimal pulses found by the GA. Bottom panel: temporal phases and intensities for the same two pulses. Black lines represent the results of a GA run at full intensity, while the red lines represent the results of a run at 20% of this intensity. Solid lines are used for intensities while dashed lines are used for the phases.

This would suggest an optimal pulse shape with structure on a timescale of several hundreds of femtoseconds.

The optimal pulse shapes from several different closed-loop learning control runs display features that are consistent with all three control mechanisms described above. They are typically over 100 fs in duration with significant temporal structure—(many optimal pulses displayed two or three subpulses with a spacing between 80 and 150 fs). Figure 5 shows two of the pulse shapes discovered in the GA experiments in both the spectral and the temporal domains. As the optimal UV pulses produce some ionization on their own, they are definitely strong enough to drive population up and down between the ground and excited states during excitation as well as dress states during wave packet evolution on the excited state. We are currently pursuing wave packet calculations and parametrized pulse shape scans to determine whether the control mechanism involves any of the possibilities above.

VI. CONCLUSION

Our measurements and calculations demonstrate how one can use strong-field dissociative ionization as a diagnostic tool for gas phase closed-loop control experiments when the different final states have identical atomic composition but different geometries. We used this technique in conjunction with shaped ultrafast laser pulses in the deep ultraviolet to demonstrate control of the ring-opening reaction in CHD. Our calculations demonstrate that we can understand the final state detection in terms of the geometry-dependent electronic structure of the molecular ion and we are currently pursuing calculations that will allow us to understand the control mechanism in detail.

ACKNOWLEDGMENTS

We gratefully acknowledge support from the National Science Foundation under Award Nos. 0555214 and 0449853 and the Department of Energy under Award Nos. DE-FG02-

08ER15984 and DE-PS02-08ER08-01. We are also very grateful to Werner Fuss for providing us with an HT sample and data.

[1] R. W. Schoenlein, L. A. Peteanu, R. A. Mathies, and C. V. Shank, Science **254**, 412 (1991).
[2] B. G. Levine and T. J. Martinez, Annu. Rev. Phys. Chem. **58**, 613 (2007).
[3] M. J. Pilling and S. Robertson, Annu. Rev. Phys. Chem. **54**, 245 (2003).
[4] W. Tsang, Data Science Journal **3**, 1 (2004).
[5] S. P. Shah and S. A. Rice, Faraday Discuss. **113**, 319 (1999).
[6] V. I. Prokhorenko, A. M. Nagy, S. A. Waschuk, L. S. Brown, R. R. Birge, and R. J. D. Miller, Science **313**, 1257 (2006).
[7] H. Tamura, S. Nanbu, T. Ishida, and H. Nakamura, J. Chem. Phys. **125**, 034307 (2006).
[8] R. S. Judson and H. Rabitz, Phys. Rev. Lett. **68**, 1500 (1992).
[9] G. Vogt, G. Krampert, P. Niklaus, P. Nuernberger, and G. Gerber, Phys. Rev. Lett. **94**, 068305 (2005).
[10] B. Dietzek, B. Bruggemann, T. Pascher, and A. Yartsev, Phys. Rev. Lett. **97**, 258301 (2006).
[11] E. C. Carroll, J. L. White, A. C. Florean, P. H. Bucksbaum, and R. J. Sension, J. Phys. Chem. A **112**, 6811 (2008).
[12] E. C. Carroll, B. J. Pearson, A. C. Florean, P. H. Bucksbaum, and R. J. Sension, J. Chem. Phys. **124**, 114506 (2006).
[13] K. Hoki and P. Brumer, Phys. Rev. Lett. **95**, 168305 (2005).
[14] W. Fuß, W. E. Schmid, and S. A. Trushin, J. Chem. Phys. **112**, 8347 (2000).
[15] P. Celani, F. Bernardi, M. Robb, and M. Olivucci, J. Phys. Chem. **100**, 19364 (1996).
[16] S. H. Pullen, N. A. Anderson, L. A. Walker II, and R. J. Sension, J. Chem. Phys. **108**, 556 (1998).
[17] A. Hofmann and R. de Vivie-Riedle, J. Chem. Phys. **112**, 5054 (2000).
[18] M. Garavelli, C. S. Page, P. Celani, M. Olivucci, W. E. Schmid, S. A. Trushin, and W. Fuß, J. Phys. Chem. A **105**, 4458 (2001).
[19] H. Tamura, S. Nanbu, T. Ishida, and H. Nakamura, J. Chem. Phys. **124**, 084313 (2006).
[20] N. Kuthirummal, F. M. Rudakov, C. L. Evans, and P. M. Weber, J. Chem. Phys. **125**, 133307 (2006).
[21] H. J. C. Jacobs and E. Havinga, Adv. Photochem. **11**, 305 (1979).
[22] B. J. Pearson and T. C. Weinacht, Opt. Express **15**, 4385 (2007).
[23] D. A. Flickinger, R. N. Coffee, G. N. Gibson, and T. C. Weinacht, Appl. Opt. **45**, 6187 (2006).
[24] R. L. Fork, O. E. Martinez, and J. P. Gordon, Opt. Lett. **9**, 150 (1984).
[25] R. Trebino, K. W. DeLong, D. N. Fittinghoff, J. N. Sweetser, M. A. Krumbugel, B. A. Richman, and D. J. Kane, Rev. Sci. Instrum. **68**, 3277 (1997).
[26] F. Langhojer, D. Cardoza, M. Baertschy, and T. Weinacht, J. Chem. Phys. **122**, 014102 (2005).
[27] H. Lischka, R. Shepard, R. M. Pitzer, I. Shavitt, M. Dallos, Th. Müller, P. G. Szalay, M. Seth, G. S. Kedziora, S. Yabushita, and Z. Zhang, Phys. Chem. Chem. Phys. **3**, 664 (2001).
[28] H. Lischka, R. Shepard, F. B. Brown, and I. Shavitt, Int. J. Quantum Chem., Quantum Chem. Symp. **15**, 91 (1981).
[29] M. W. Schmidt, K. K. Baldridge, J. A. Boatz, S. T. Elbert, M. S. Gordon, J. H. Jensen, S. Koseki, N. Matsunaga, K. A. Nguyen, S. Su, T. L. Windus, M. Dupuis, and J. A. Montgomery, J. Comput. Chem. **14**, 1347 (1993).
[30] B. J. Pearson, S. R. Nichols, and T. Weinacht, J. Chem. Phys. **127**, 131101 (2007).
[31] R. C. Dunbar and H. H.-I. Teng, J. Am. Chem. Soc. **100**, 2279 (1978).
[32] M. Allan, J. Dannacher, and J. P. Maier, J. Chem. Phys. **73**, 3114 (1980).
[33] M. P. Fulscher, S. Matzinger, and T. Bally, Chem. Phys. Lett. **236**, 167 (1995).
[34] M. V. Ammosov, N. B. Delone, and V. P. Krainov, Sov. Phys. JETP **64**, 1191 (1986).
[35] D. Geppert and R. de Vivie-Riedle, Chem. Phys. Lett. **404**, 289 (2005).